AFRL-AFOSR-JP-TR-2024-0055

Non-Intrusive, Reliable, and Portable Laser Induced Breakdown Spectroscopy for Instantaneous Gas Composition and Density Measurements in High-Speed Flows

Do, Hyungrok
SEOUL NATIONAL UNIVERSITY
1, GWANAK-RO, GWANAK-GU
SEOUL, ,
KOR

02/25/2024
Final Technical Report

Air Force Research Laboratory
Air Force Office of Scientific Research
Asian Office of Aerospace Research and Development
Unit 45002, APO AP 96338-5002

REPORT DOCUMENTATION PAGE

PLEASE DO NOT RETURN YOUR FORM TO THE ABOVE ORGANIZATION.

1. REPORT DATE	2. REPORT TYPE	3. DATES COVERED	
20240225	Final	START DATE 20200918	END DATE 20230917

4. TITLE AND SUBTITLE
Non-Intrusive, Reliable, and Portable Laser Induced Breakdown Spectroscopy for Instantaneous Gas Composition and Density Measurements in High-Speed Flows

5a. CONTRACT NUMBER	5b. GRANT NUMBER	5c. PROGRAM ELEMENT NUMBER
	FA2386-20-1-4054	
5d. PROJECT NUMBER	**5e. TASK NUMBER**	**5f. WORK UNIT NUMBER**

6. AUTHOR(S)
Hyungrok Do

7. PERFORMING ORGANIZATION NAME(S) AND ADDRESS(ES)
SEOUL NATIONAL UNIVERSITY
1, GWANAK-RO, GWANAK-GU
SEOUL
KOR

8. PERFORMING ORGANIZATION REPORT NUMBER

9. SPONSORING/MONITORING AGENCY NAME(S) AND ADDRESS(ES)	10. SPONSOR/MONITOR'S ACRONYM(S)	11. SPONSOR/MONITOR'S REPORT NUMBER(S)
AOARD UNIT 45002 APO AP 96338-5002	AFRL/AFOSR IOA	AFRL-AFOSR-JP-TR-2024-0055

12. DISTRIBUTION/AVAILABILITY STATEMENT
A Distribution Unlimited: PB Public Release

13. SUPPLEMENTARY NOTES

14. ABSTRACT
The original design of the gas property monitoring system is illustrated in Fig. 1. There are two separate measurement domains considered for the design; (1) Cold (unburned) Flow Region and (2) Hot (burned) Flow Region.
In the Region (1), ps-LIBS or chopped ns-LIBS is proposed for measuring the gas density, species concentration, and velocity in the intake and isolator area since there is no photon source (within UV, VIS, and NIR for easy detection) in cold flows. For improving the accuracy and extending the possible measurement conditions of the ns-LIBS, the ns laser pulses are modulated, and data-driven machine learning techniques are employed. However, the LIBS measurement inherently requires relatively high laser pulse energy for inducing the breakdown. In addition, a diode laser with a set of guide optics is essential for the velocity measurement using LIBS as tested in the first project year. Interestingly, particularly in the supersonic flows, the SRBS signal is found to be sensitive to the flow speed, therefore, the SRBS signal can also be used for estimating the flow velocity although the LIP-induced shockwave velocimetry (LIPSV) developed in the first project year is more accurate velocity measurement method. We will continue to improve the SRBS velocimetry in a future work. The SRBS signal is fine resolved by a minimal-sized VIPA to be calibrated with gas density and discern molecular species. It is shown that, at least with a limited number of molecular species, the SRBS can be used for gas density and composition measurements. In short, the measurement system in the Region (1) can be further simplified with the SRBS method implemented with a low power laser source, a minimal-sized VIPA optics, and a 2D CCD array chip, e.g., a quarter square inch panel for 1024 by 1024 pixels, to image the 2D SRBS signal.
In the Region (2), the flame emission spectroscopy (FES) aided by the POD calibration and physics-guided denoising CNN is proven to be the simplest and accurate gas property monitoring method in the combustion region. The spontaneous photon emissions from the reaction regions contain such quantitative property information, and a miniaturized small spectrometer is found to be sufficient to capture the flame emission characteristics. Therefore, a tiny spectrometer with a data processing unit would be enough to provide the combustor operation conditions essential for vehicle control, which includes local fuel concentration, flame temperature, and gas density. Local concentration of molecular oxygen could also be measured using the two-delay LIBS developed in this research project, that records oxygen absorption lines in the early plasma stage later with the atomic emission lines. Nevertheless, the oxygen absorption line measurement requires a high-resolution spectrometer of a long focal length with a signal intensifier. Therefore, the two-delay LIBS is inappropriate for the onboard system although the absorption spectroscopy is an effective method estimating molecular oxygen concentration indicating local combustion reaction progress.
Consequently, the proposed gas property measurement system consists of 1) a tiny single optical access or optical cable for each of the inlet-isolator and engine, 2) a portable low-resolution spectrometer for FES, 3) a low-power laser source inducing SRBS, 4) minimal-sized VIPA optics set, 5) a CCD array chip, and 6) a signal processor converting the optical signals to the gas properties of interest including I) density (temperature with pressure information), II) gas composition, and III) velocity. Among the various optical measurement methods tested in the research project, 1) fast FES with POD-guided Machine Learning & Denoising and 2) SRBS are chosen for the onboard gas property monitoring system.

15. SUBJECT TERMS

16. SECURITY CLASSIFICATION OF:			17. LIMITATION OF ABSTRACT	18. NUMBER OF PAGES
a. REPORT	b. ABSTRACT	c. THIS PAGE		
U	U	U	SAR	28

19a. NAME OF RESPONSIBLE PERSON	19b. PHONE NUMBER *(Include area code)*
TODD RUSHING	315-227-7003

Final Report [FA2386-20-1-4054]

NON-INTRUSIVE, RELIABLE, AND PORTABLE LASER INDUCED BREAKDOWN SPECTROSCOPY FOR INSTANTANEOUS GAS COMPOSITION AND DENSITY MEASUREMENTS IN HIGH-SPEED FLOWS

December 2023

Submitted to:
Asian Office of Aerospace Research and Development
AOARD PO: Todd Rushing
AFRL POC: Campbell D. Carter

Submitted by: **Hyungrok Do**
Professor, Department of Mechanical Engineering
Seoul National University
Room 1518 Bldg 301 Kwanak-ro 1 Kwanak-gu Seoul
South Korea 08826
Office: +82 2 880 1597, Cell: +82 10 7129 0656

TABLE OF CONTENTS

1. OBJECTIVES

The proposed work aims to develop a flexible and portable n-LIBS fuel-air sensor for accurate gas property measurements in high-speed compressible reacting flows.

The main objective of the proposed work is to facilitate applications of the n-LIBS measurement technique to real test environments and improving its measurement accuracy and reliability.

1. ***Objective 1: Develop flexible and portable n-LIBS fuel-air sensor***
    - Miniaturization of current instrument
    - Optimization of pulse properties using pulse-shaping approaches
    - Investigation of window damage from n-LIBS
2. ***Objective 2: Improve sampling rate and measurement accuracy***
    - Exploration/extension of sampling rate
    - Exploration of enhancement to DSM fitting to improve measurement accuracy
3. ***Objective 3: Measure gas properties in Air Force relevant conditions***
    - Improvement in instrument for testing in air force relevant conditions

In the second project year (Sept. 1, 2021 – Aug. 31, 2022), most of the research activities have been focused on: **1) improving sampling rate and measurement accuracy,** and **2) measuring gas properties in Air Force relevant conditions**. **Proper orthogonal decomposition (POD) and machine learning (ML) techniques** were employed to improve the temporal resolution of the optical gas property measurement methods developed in the first project year, and **preliminary gas property measurements in high-speed and high-pressure environments** under Air Force relevant conditions were conducted. In addition, **3) a new application of the LIBS for estimating the local combustion efficiency** was proposed and laboratory scale proof-of-concept experiments were conducted.

2. PROPOSED RESEARCH ACTIVITIES

Objective 1 – Develop Flexible and Portable n-LIBS Fuel-Air Sensor

<u>Tasks of Objective 1</u>

1.a Install an injection-seeder on a Nd:YAG laser. Focus fundamental, second-, third-, and fourth-harmonic laser pulses of the Nd:YAG to generate plasma shutters of different characteristics. *(month 1 – 6):* ***Completed***

1.b Design and make a pressure cell of variable pressure and gas species conditions to precisely control the characteristics of the plasma shutter. Try various combinations of saturable absorbers and beam expanders in the upstream of the pressure cell to modulate ns laser pulses with improved pulse energy conversion efficiency. *(month 3 – 12):* ***Completed***

1.c Test DPSS laser sources with a CW laser as a subsidiary photon energy source. *(month 13 – 24):* ***Completed***

1.d Measure MPE and PEA at Air Force relevant gas conditions with the modulated laser pulses of different laser pumping sources. *(month 19 – 24):* ***Completed***

1.e Inject modulated pulses through an optical access window with varied focal length, pulse energy, and profile to investigate window damage. *(month 19 – 30)* ***Completed***

Objective 2 – Improve Sampling Rate and Accuracy

Tasks of Objective 2

2.a Collect plasma emission spectra with modulated pulses. *(month 7 – 24):* ***Completed***

2.b Explore possible use of low pulse energy laser sources. *(month 13 – 24):* ***Completed***

2.c Improve DSM database with two separate emission spectra captured at two different delays. *(month 19 – 30)* ***Completed***

Objective 3 – Testing in Air Force Relevant Conditions

Tasks of Objective 3

3.a Measure gas property using the new n-LIBS in a small-scale supersonic wind tunnel at SNU. *(month 24 – 36)****: Completed***

3.b Make the n-LIBS system as compact as possible. *(month 24 – 30)* ***Completed***

3.c Measure gas property using the compact n-LIBS system in a high-pressure swirl combustor and a supersonic wind tunnel at SNU. *(month 31 – 36)* ***Completed***

3. YEAR-1 RESULTS

1) Preliminary design of the n-LIBS fuel-air sensor

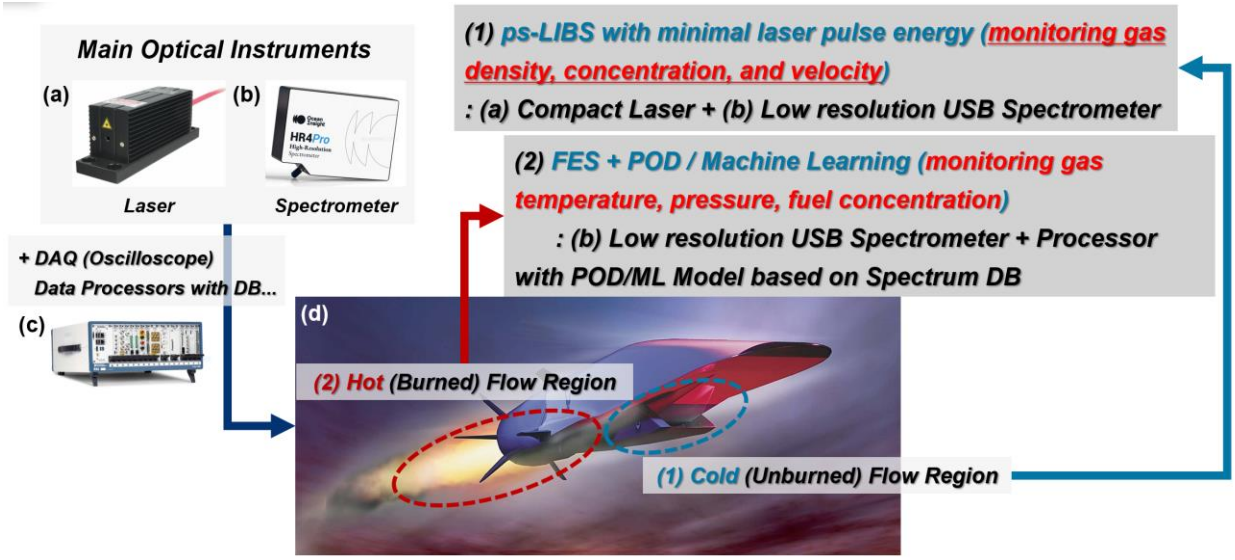

Figure 1 Preliminary design of the compact n-LIBS air-fuel sensor system

Figure 1 overviews the preliminary design of the n-LIBS fuel-air sensor. The sensor system has been developed for monitoring the gas composition, density, temperature, and flow velocity in the cold (unburned) flow region as well as the hot (burned) flow region. The primary goal of the

design is to make the system compact and accurate in both the flow conditions, which is challenging since the gas property and velocity is quite different in the two regions. Therefore, two separate solutions were proposed as illustrated in Fig. 1.

(1) *Cold flow region*: ps-LIBS with minimal laser pulse energy for monitoring gas density, concentration, and velocity

System components: Low power compact laser + Low resolution compact spectrometer + Diode laser and a fast-photodiode

(2) *Hot flow region*: FES (flame emission spectroscopy) + proper orthogonal decomposition (POD) / Machine Learning (ML) (monitoring gas temperature, pressure, fuel concentration)

System components: Low resolution compact spectrometer + Processor with POD/ML Model based on spectrum DB

In the cold flow region after the inlet compression, the gas density is high and the gas temperature is relatively low. Fuel is typically injected upstream of the combustion region after the inlet compression for enhancing the fuel-air mixing and combustion. Consequently, high-density flammable mixtures moving at a supersonic speed should be monitored for providing critical engine operation parameters. Laser-pulses of relatively low pulse energy (< 5 mJ/pulse) and short pulse width (pulse width < 1 ns) will be focused into the cold flow for generating laser-induced plasmas (LIP) that emit photons containing gas property information. As we have shown in our previous collaborations with Dr. Campbell D. Carter at Air Force Research Laboratory (AFRL), the ps-LIBS is a non-intrusive gas property measurement method applicable to highly-flammable gas mixtures. More importantly, the power requirement for generating the ps-LIP is significantly low enabling the use of compact laser systems, e.g., compact microchip lasers.

The other critical component of this sensor system is the low-resolution compact spectrometer. In general, low-resolution compact spectrometer with a simple USB connection is improper for accurate LIBS measurements. However, our year-1 research utilizing the POD and ML techniques confirmed that the low-resolution spectra contain sufficient information for accurately estimating the target gas properties. This is because the POD and ML take the entire spectrum profile to predict the corresponding gas properties, while only selected spectrum features such as the atomic emission lines were correlated with the gas properties in conventional LIBS measurements.

The POD and ML can also be used for measurements in high-temperature combustion products. In the hot gas condition, the gas density drops significantly due to the increased gas temperature from the combustion heat release. Under the low-density conditions, laser-induced breakdown requires much higher photon energy, e.g., > 100 mJ/pulse with ns-laser pulses, which is impossible to achieve with compact microchip lasers, at most a few mJ/pulse. Since the primary goal of this project is to miniaturizing the sensor system, including a large high-power pulsed laser is inappropriate. Alternatively, spontaneous emission from the high-temperature gas can be used for estimating the gas properties in the region. Particularly, flame emission spectroscopy (FES) can be employed to obtain quantitative gas property information. However,

the measurement accuracy of the FES is relatively low in comparison with LIBS techniques. In our year-1 research, it was confirmed that the spontaneous emission spectrum can be accurately correlated with the gas properties of interest when aided by the POD and ML methods. Some more details regarding the spectrum analyses will be described later in this report; I) spectrum databases for LIBS and FES were collected, II) the spectrum profiles were decomposed, and III) the decomposed components form a model predicting the gas properties utilizing the ML or POD (Kriging) model algorithm. The POD or ML models with the spectrum database can conveniently be embedded on a processor chip to be used for the portable sensor system.

In short, the sensor system will consist of a processor chip with the spectrum database, a compact microchip laser + a diode laser, and a compact USB spectrometer with a data acquisition system transferring the input spectra to the processor. The output of the sensor system would be the gas properties in the upstream and downstream regions of the combustion zone and the flow velocity of the inlet-compressed air with fuel.

2) Improvement of the measurement accuracy: proper orthogonal decomposition (POD) method and machine learning technology (ML)

The POD and ML techniques were utilized to improve the measurement accuracy of the FES and LIBS measurements. The most prominent merit of these techniques comes from the systematic extraction of gas-property-sensitive components hidden in the overall spectrum profile, not limited to a few specific spectral features. In conventional spectrum analyses, specific spectral features observed in the emission spectra were theoretically investigated to provide correlations of the features, e.g., emission line strength and width, and measurement target gas properties. For example, emission line width, peak intensity, and broadband emission strength have been measured to estimate electron number density/temperature, atom number density, electron/molecular number density, etc. See below the theoretical expressions of the emission line and broadband emission profiles with the SAHA equilibrium equation that is used for simplifying the theoretical property-to-spectral feature correlations.

Line Emission
$$\varepsilon_l(\nu) = \frac{h\nu}{4\pi} A_{21} \frac{g_2}{2U_i} \frac{h^3}{(2\pi m k)^{\frac{3}{2}}} n_e n_i T_e^{-\frac{3}{2}} \left[\exp\left(\frac{E_i - E_2 - \Delta E_i}{kT_e}\right)\right]$$

Broadband Emission
$$\varepsilon_c(\nu) = \left(\frac{16\pi e^6}{3c^3(6\pi m^3 k)^{\frac{1}{2}}}\right) \frac{n_e n_i}{T_e^{\frac{1}{2}}} \left[\xi\left(1 - \exp\frac{-h\nu}{kT_e}\right) + Gexp\frac{-h\nu}{kT_e}\right]$$

SAHA Eq. Equation
$$\frac{n_e n_i}{n_a} = \frac{2Z_i}{Z_a} \frac{(2\pi m k T_e)^{\frac{3}{2}}}{h^3} \left[\exp\left(-\frac{E_i - \Delta E_i}{kT_e}\right)\right]$$

However, temporally evolving electron temperature, electron number density, recombination reactions, and energy transfer to the surroundings all affect these correlations, therefore, the accuracy of the property measurements strongly depends on measurement conditions and measurement devices used to collect the spectra. This is the primary reason to use high-resolution spectrometers, short-gated high-sensitivity photon collectors, high-power injection-seeded pulsed-lasers, and high-precision time scheduling devices for the conventional LIBS to improve the measurement accuracy.

The POD and ML mathematically decompose the entire spectrum profile to extract multiple parameters sensitive to the target gas properties. Therefore, the POD and ML do not rely on local spectrum features or accuracy of their specific dimensions. In order to estimate the gas properties more accurately using the novel methods, the captured spectral range needs to be extended since the spectrum will contain more emission lines, bands, systems, and overall broadband profiles over a broader spectral range. Compact low-resolution USB spectrometers work perfectly for this purpose.

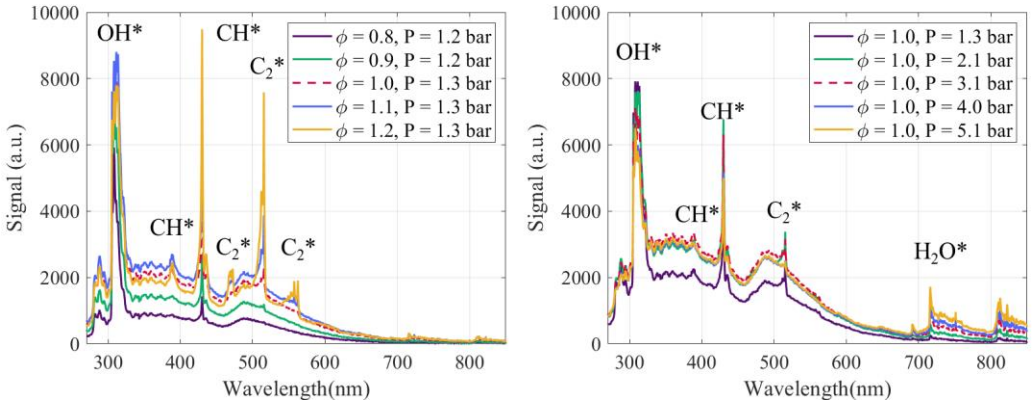

(a) **(b)**

Figure 2 Flame emission spectra with varied fuel concentration in air and ambient pressure

Figure 2 presents flame emission spectra with varied ambient pressure and fuel concentration in air. Conventional FES measures the emission line intensities and their ratios as the fuel concentration indicators, and the line intensity to the broadband strength ratio at a specific location was used as a gas density indicator. As mentioned earlier, these quantities measured in a very narrow spectral range strongly depend on the test conditions and the specifications of the measurement devices such as the resolution of a spectrometer and the photosensitivity of a camera that is in fact a function of wavelength.

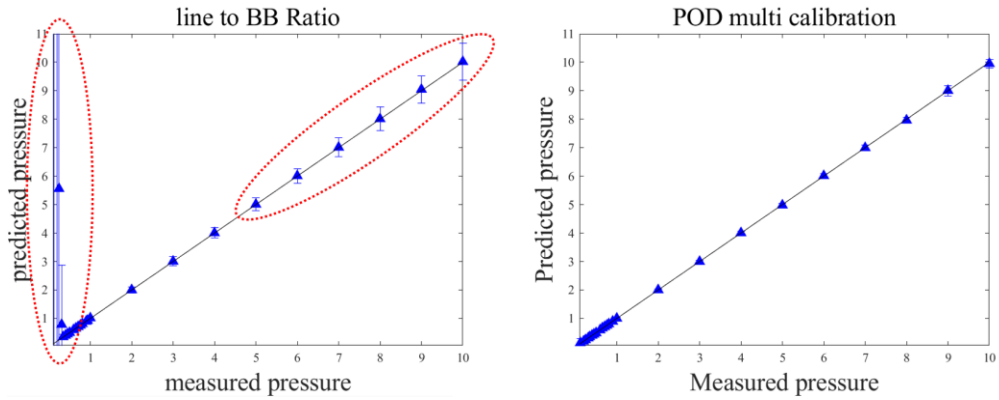

(a) **(b)**

Figure 3 (a) conventional pressure (gas density) estimation employing the emission line to broadband strength ratio, and (b) POD pressure prediction using the same spectrum database

Figure 3(a) clearly describes the limitation of the conventional technique being remarkably influenced by the ambient measurement condition; the pressure prediction accuracy gets significantly worse near the lower pressure bound below 0.5 bar and above 5 bar ambient pressure. This is due to the nonlinear response of a specific spectral feature to the ambient pressure variation in the range. For example, the near IR region between 700 – 800 nm is highly sensitive to the ambient pressure at the elevated pressure condition (see Fig. 2(b)), however, the near UV broadband emission profile becomes dominant in relatively low-pressure conditions while the spectrum in the near IR region is nearly undetectable (Fig. 2(a)). Consequently, when choosing a specific spectral feature as a pressure indicator in a certain pressure range, e.g., the H_2O band strength in high pressure conditions, it will not work in a different pressure ranges, e.g., under the pressure below 1 bar.

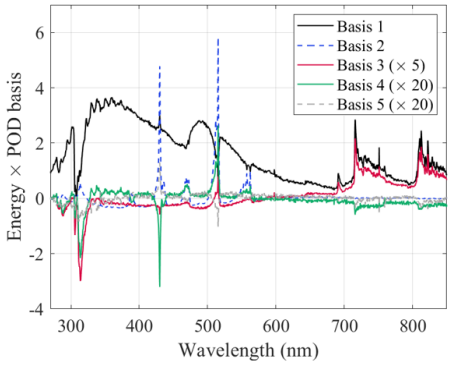

Figure 4. POD components extracted from a FES database

On the contrary, the prediction accuracy is significantly improved in the entire ambient pressure range when employing POD (Fig. 3(b)). This is because the POD extracts pressure sensitive components from the whole spectrum range. Figure 4 graphically illustrates the POD components, bases 1 – 5, that are extracted from a flame emission spectrum database previously constructed via calibration experiments under well-known ambient pressure and fuel concentration conditions. The Basis 1 containing the broadband emission profile over the entire spectral range represents the gas density or ambient pressure, the Basis 2 consisting of sharp emission peaks is highly sensitive to species concentration, and the Basis 3 describes the dependency of the spectrum on elevated pressure conditions. This observation is confirmed in the sensitivity index analyses shown in Fig. 5. The Basis 1 is the dominating factor determining the ambient pressure with non-negligible contribution of the Basis 3, and the Basis 2 is the component mostly responsible to the fuel concentration. These POD components were then combined to form a surrogate model (Kriging model) for estimating the ambient pressure and fuel concentration taking a low-resolution spectrum captured by a USB spectrometer as the input. Figure 6 confirms that this surrogate model provides significantly improved accuracy of the FES measurement results.

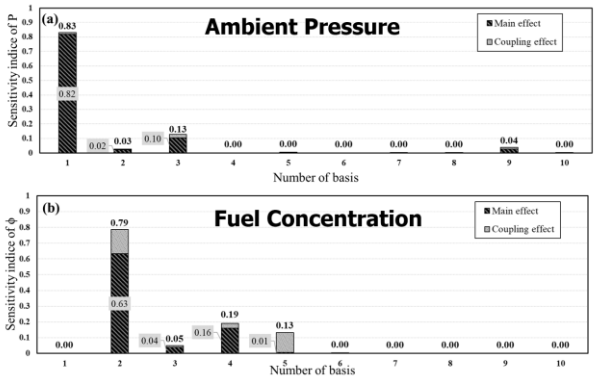

Figure 5. Contribution of each POD components to the prediction of ambient pressure and fuel concentration

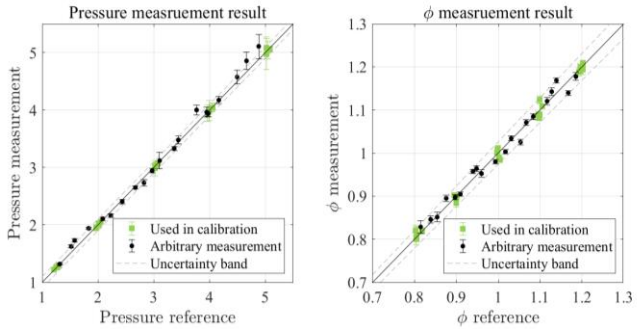

Figure 6. High-accuracy FES measurements with POD

Similar techniques can be used for LIBS to improve the measurement accuracy once an intensive LIP spectrum database is provided. Alternatively, a machine learning technique with principal component analysis (PCA) and independent component analysis (ICA) for extracting the gas property sensitive components was employed for LIBS in this research project. The decomposed components were used to build an extreme learning machine (ELM) model trained with the spectrum database. The model prediction of the pressure and fuel concentration was found be highly accurate approaching the limit of uncertainty range determined by the measurement devices (see Fig. 7 below).

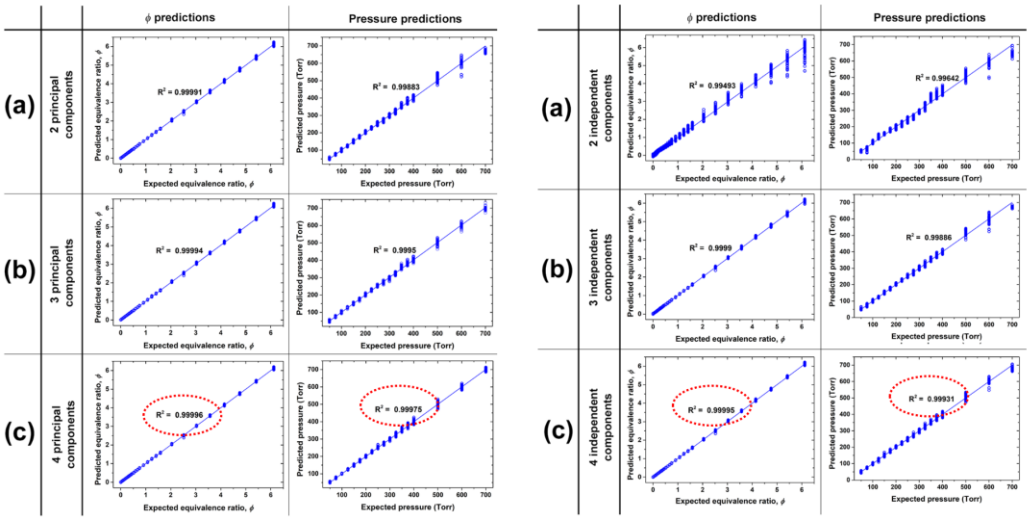

Figure 7 Improved LIBS measurement accuracy with ML

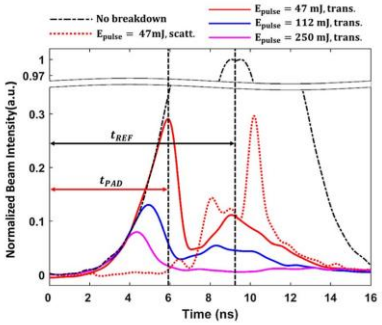

Figure 8. Pulse profiles transmitted through and scattered on a LIP

3) Laser pulse modulation technique: optical cell species variation

In our previous investigations, compressed air has been used for ns-laser pulse modulation. Molecular nitrogen, N_2, is the dominant species in Air, therefore, N_2 ionization characteristics primarily determines the laser-induced breakdown behavior and the pulse chopping capability of the LIP. Recall that the inverse-Bremsstrahlung (IB) fast photon absorption triggers intense electron production to immediately stop the transmission of a laser pulse through the LIP. Therefore, the LIP inducing the IB process has been used as a fast-optical shutter to modulate ns-laser

pulses. However, the molecular nitrogen in the plasma undergoes complex ionization, dissociation, and recombination processes, which make it difficult to define a dominant ionization pathway after the IB process is activated, particularly in the presence of oxygen molecules. Figure 8, pulse profiles transmitted through a LIP generated in air, indicates that the pulse transmission through the plasma was not completely stopped after the IB-activation. There could be various reasons of this observation including fast electron diffusion, electron-recombination, molecular dissociation, energy transfer to the surroundings, etc., which would be significantly influenced by the ambient conditions such as the pressure, temperature, and ionization potentials of the dissociated atoms/molecules. Moreover, the molecular species have rotational and vibrational modes that can generate nearly infinite number of energy states. In short, fine control of the plasma behavior is impossible.

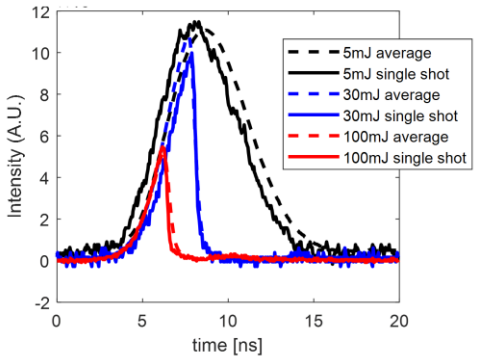

Figure 9. Instantaneous sharp cut of ns-laser pulses with Ar instead of air accommodating the LIP induced for pulse chopping.

Alternatively, noble gas species, i.e., having only electronic internal energy mode, can be used for the same purpose with improved shutter control capability. Dissociation of molecules and ionization of the dissociated particles will not happen with noble gas, and only a few selected electronic excitation states will be allowed under a given plasma condition. Figure 9 shows remarkably improved pulse chopping capability with compressed Ar in an optical cell. As experimentally revealed in our previous work, the pulse chopping time could be effectively controlled by adjusting the pulse energy, pulse rise time, and the gas pressure in the optical pressure cell. With the remarkably improved pulse chopping capability, fine pulse modulation control was enabled.

4) Electron-seeding breakdown

We have planned to use a focused continuous laser to lower the LIP breakdown threshold. A kW-level high-power CO_2 laser was used for the proof-of-concept. However, the threshold reduction was not noticeable in the first trial, and possible reasons of the failure need to be identified in the future. In the process of the preliminary testing, however, it became clear that the use of the large high-power CO_2 laser will make the sensor system bigger, which is obviously not desirable in this research project. Therefore, we decided not to include the continuous laser in the sensor system.

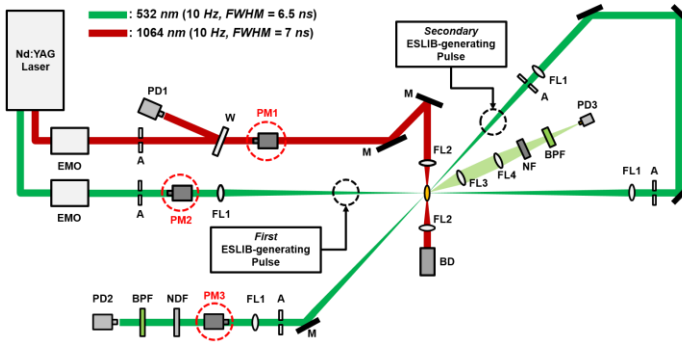

Figure 10. Electron-seeding controlled pulse modulation setup

Alternatively, we have devised a new concept, electron-seeding breakdown. There are several ways of generating free electrons in the atmosphere, e.g., applying strong electric potential to produce weakly

ionized gas and optical breakdown with focused high-power laser pulses. For a preliminary investigation, 1064-nm laser pulse split before frequency-doubling was focused to generate a plasma, i.e., an auxiliary breakdown for electron seeding (ALIB), and later the frequency-doubled 532-nm pulse was focused near the ALIB area (see the experimental setup in Fig. 10). The 532-nm pulse arrival time at the ALIB location could be adjusted by extending or shortening the 532-nm beam path, and the focal point of the 532-nm beam relative to the ALIB location was varied to systematically investigate the effect of electron-seeding; recall that the electron number density in the ALIB is highly non-uniform. It is evident that the IB induction by the focused 532-nm beam can be controlled with varied electron seeding, and the breakdown threshold could be significantly reduced.

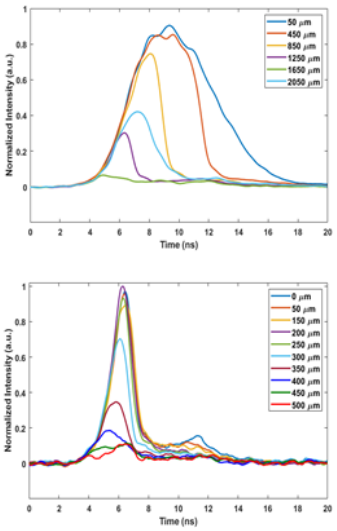

Figure 11. Pulse modulation with electron-seeding; (upper) first transmission, and (lower) second transmission

This electron-seeding strategy can be employed in two different ways for achieving the goal of this research project; 1) pulse modulation and 2) multi-beam focusing for breakdown threshold reduction. The IB-induction time or pulse chopping time can be controlled by the seeding-electron density independent of the pulse energy and ambient gas conditions. Therefore, the pulse width and pulse energy can be separately controlled regardless of the ambient pressure; location of the 532-nm beam relative to the ALIB was adjusted to vary the seed-electron number density and the resulting pulse profile of the transmitted beam as shown in Fig. 11. The 532-nm beam passed the ALIB region twice to carve the pulse profile twice. The breakdown of the focused 532-nm beam was not observed without the electron-seeding from ALIB confirming that the breakdown threshold was lowered. In addition, the ALIB plasma region was significantly expanded after the transmission of the converging 532-nm beam indicating that the electron seeding can amplify the plasma strength. Likewise, weak initial breakdown induced by a low-energy sub-ns pulse can be amplified by another low-energy laser pulses, either of ns- or ps-pulses. Consequently, proper combinations of low-energy pulses from compact lasers would be able to sustain intense plasmas, which is beneficial for obtaining high SNR emission signals.

5) Flow velocity measurements using laser-induced breakdown

Velocity measurements using LIP were not originally planned in the proposal. We have accidentally found that the LIP-induced shockwave can be accurately detected with a low power diode laser which was installed initially for laser absorption spectroscopy. We have reconfigured the setup for tracking the LIP-induced shockwave; two parallel probe beams (one reciprocating beam traversing the region twice) near the LIP were guided to a fast-responding photodiode. This enables accurately measuring the velocity of the ambient flow that carries the shockwave. Evolution of the LIP-induced shockwave could be well predicted by a semi-empirical point-explosion model, e.g., the radius of the shock as a function of time, and the shock-arrival time on the two probe beam locations were recorded to calculate the ambient flow velocity. One probe

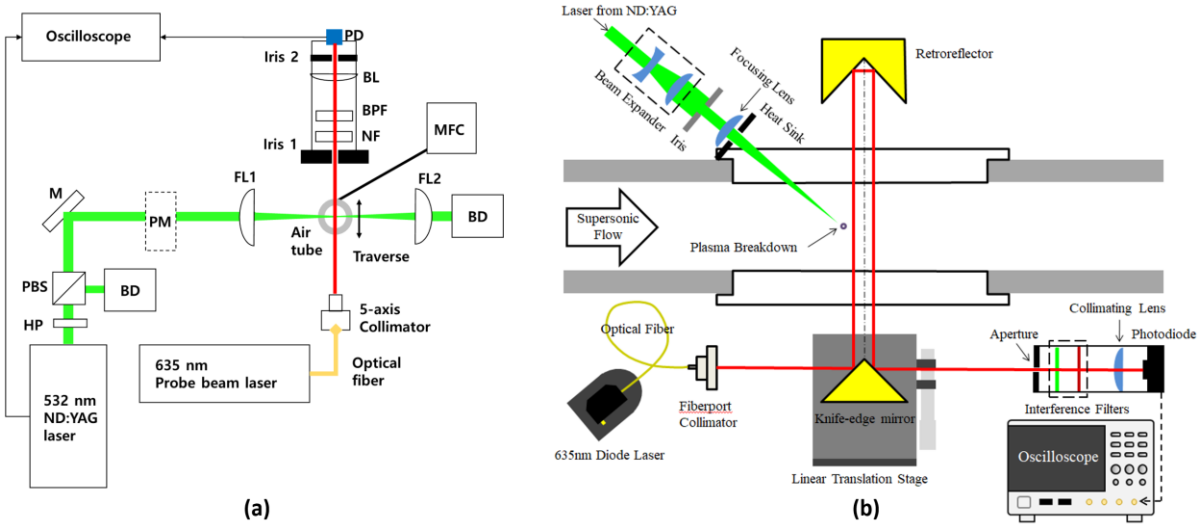

Figure 12. LIP flow velocimetry in (a) subsonic and (b) supersonic flows

beam was sufficient in subsonic flows for estimating the flow velocity (Fig. 12(a)), while two were required in supersonic flows (Fig. 12(b)) since the upstream propagating shock (-shock) returns due to rapid shock deceleration after its generation on LIP (Fig. 13).

Four probe beam signal disturbances corresponding to the shock positions illustrated in Fig. 14 were recorded. The disturbance signals were then used to determine the coefficients of the shock propagation model and the flow velocity. Figure 15 shows the velocimetry test results in (a) subsonic and (b) supersonic flows. The LIP was moved to scan the velocity profile across the subsonic and supersonic flow areas. The black dotted lines represent the flow velocity estimated indirectly based on the flow rates, flow channel cross sectional area, static/stagnation pressures and temperature. The measurement uncertainty was estimated to be within 10 m/s in the supersonic flows. Most macroscopic flow features were well resolved with the velocimetry while not requiring particle seeding nor probe insertion. Alignment of the reciprocating probe beam is tricky but demanding only a single diode laser to make the system simpler. We have also tested non-parallel multi-probe laser configurations for 2D and 3D velocity component measurements.

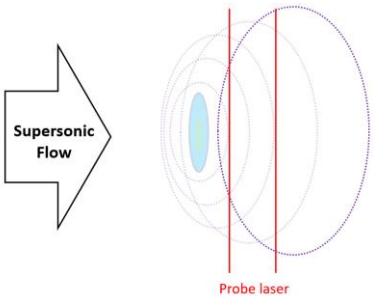

Figure 13 LIP-induced shockwave propagation in a supersonic flow. The upstream propagating shock (-shock) returns to touch the beams

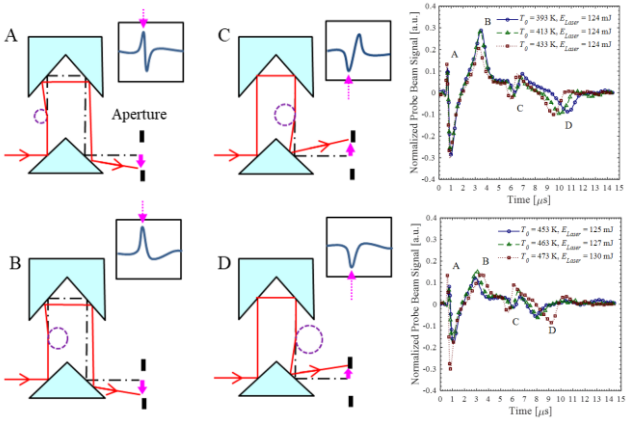

Figure 14 Shock arrival on probe beams and corresponding signals

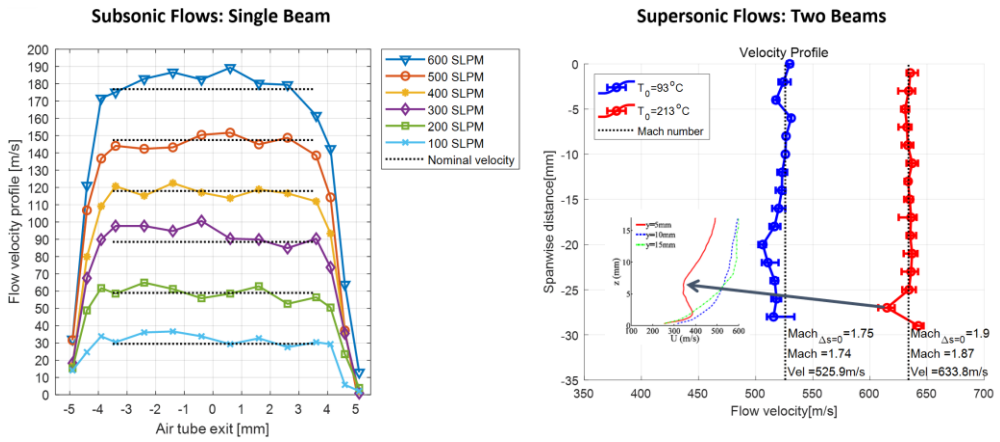

Figure 15 LIP-induced shock velocimetry provides absolute velocity at the location of the LIP: (a) subsonic and (b) supersonic flows

4. YEAR-2 RESULTS

1) Improve Sampling Rate and Measurement Accuracy

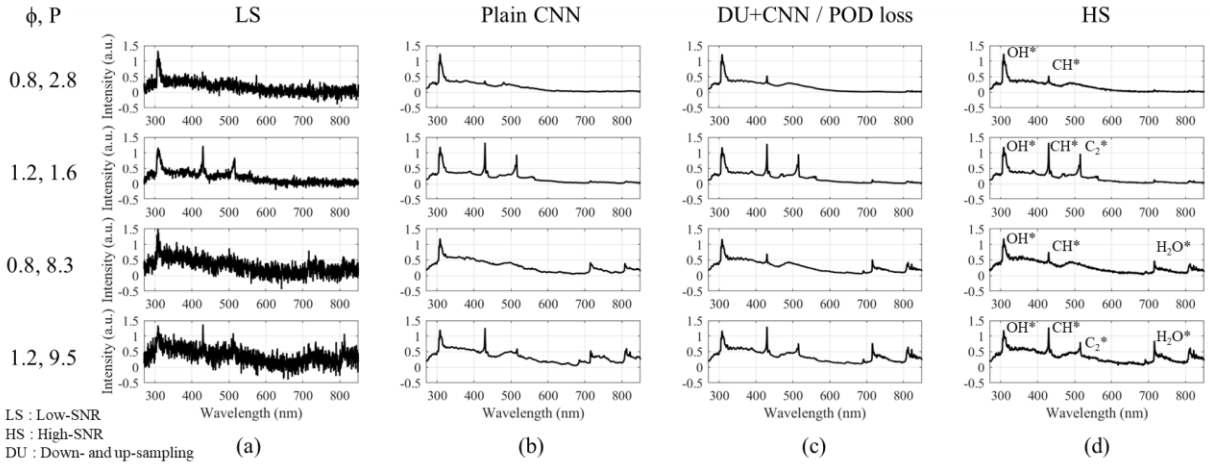

Figure 66 Performance of the newly proposed denoising CNN

In the first project year, flame emission spectroscopy (FES) with proper orthogonal decomposition was proposed and tested to minimize the volume and weight of the onboard gas property monitoring system. FES is the simplest optical gas property measurement method, which does not require the use of photon sources such as lasers or LED while spontaneous flame emissions should be collected with reasonable signal-to-noise ratio (SNR). In addition, the proposed POD-assisted non-linear modelling method for calibrating the flame emission spectra with gas properties could effectively improve the FES measurement accuracy. Nevertheless, the POD analyses for accurate gas property measurements using FES require high SNR spectrum signals that demand for long exposure of photon detectors. This will limit the temporal resolution thus the sampling rate of the measurement technique.

In the second project year, a novel denoising convolutional neural network (CNN) architecture is proposed to improve the temporal resolution of the FES measurements, i.e., accurate measurements with reduced exposure of photon detectors. A common light-weight USB type spectrometer is used for miniaturizing the measurement system, and the exposure time of the spectrometer is significantly reduced below one tenth of the common exposure essential for recording high SNR spectrum signals. Consequently, instrumental noise level rises to remarkably lower the SNR of the collected flame emission spectra which is proportional to the square root of the exposure time, therefore, the FES measurement accuracy becomes worse. The proposed denoising CNN architecture removes the random instrumental noise without losing critical spectral features sensitive to the gas properties. A down- and up- sampling (DU) operator and a modified loss function considering POD loss are employed to guide the denoising process customized for the flame emission spectrum analyses.

Figure 16 demonstrates the improved denoising capability of the combination of DU + CNN architecture and the loss function containing the POD loss term. The spectra used here to test the new CNN model are from the test dataset that was not used to train the model. This is to confirm the performance of the model taking the input of arbitrary unknown chemiluminescence signals. The chemiluminescence spectra acquired for 0.2 s and 2 s exposure are shown in Figs. 1 (a) and (d), which are denoted as low-SNR (LS) and high-SNR (HS), respectively. Characteristic local spectral features from excited molecules are clearly observed in the HS spectra (Fig. 1(d)) including OH* at 306.4 nm, CH*at 431.4 nm, C2* swan bands at 517 nm, and H2O* at 700 – 850 nm. The strength and shape of the spectral features and the broadband background emission profile over the entire spectrum range are highly dependent on the gas properties in and near the combustion reaction zone and the chemical reactions in progress. Therefore, reconstructing the shape of the features accurately from LS signals is critical for improving the measurement accuracy with reduced exposure.

Figures 16 (b) and (c) present the outputs of a plain CNN without DU operator trained by a loss function considering only MSE (mean square error) loss and the proposed DU + CNN trained by the combination of MSE and POD loss, which are denoted as plain CNN and DU + CNN / POD loss, respectively. The two models were trained using the same sets of training and validation data. Obviously, both CNN architectures could significantly lower the noise level of the spectra compared to the short-exposure noisy input signals in Fig. 16 (a). Nevertheless, the relatively weak characteristic spectral features, such as CH* at lean conditions and H_2O* emission bands at high-pressure conditions, that are denoised by the plain CNN model (Fig. 16 (b)) are different from them in the corresponding HS spectra (Fig. 16 (d)). Recall that the HS spectra is regarded as the ground truth signals. Considering that the CH* and C_2* bands are highly sensitive to the fuel concentration (ϕ) and the H_2O* bands are the most prominent pressure indicator, the gas property prediction with the plain CNN model denoising the LS spectra would be inaccurate and biased.

On the other hand, the spectra denoised by the DU + CNN / POD loss are quite well matched with the HS spectra in most details. The noise of the input LS spectra could be successfully suppressed without missing the critical spectral features under various gas property conditions regardless of the noise level with the DU operator. We conjecture that this is because of proper down-sampling that makes a wider receptive field, which is the number of input pixels

involved to produce one output pixel, and the CNN architecture regularized by POD loss. In other words, each pixel of the output signal is denoised and reconstructed by global spectral features of the input signal with a large receptive field and guided by the POD coefficients of each basis mode. Therefore, the successful denoising process is enabled by the model decoupling the property-sensitive spectral features from the noise signal.

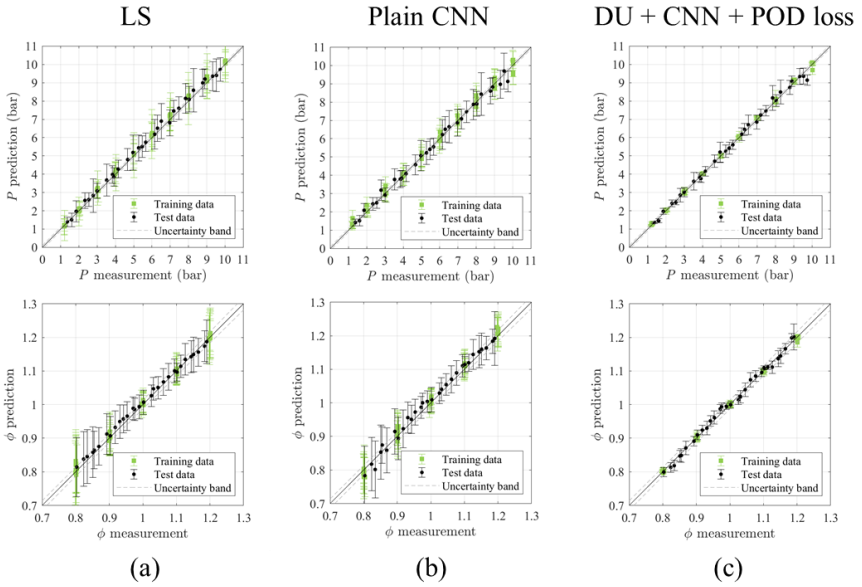

Figure 17 Pressure (P) and equivalence ratio (ϕ)-prediction using (a) low-SNR (LS) spectra, (b) output using plain CNN, and (c) output using DU + CNN / POD loss.

Figure 17 demonstrates the improved measurement accuracy utilizing the proposed CNN architecture with reduced exposure time. The plain CNN could reduce the noise level as shown Fig. 16, however, the measurement accuracy was not improved much since the property sensitive spectral features are deformed or lost in the denoising process. It is clear that the proposed CNN, DU + CNN + POD loss, outperforms the plain CNN and potentially improve the temporal resolution and accuracy of fast FES.

2) Measuring gas properties in Air Force relevant conditions

Measurement techniques, e.g., ns-pulse modulation for LIBS (laser induced breakdown spectroscopy) and seedless velocimetry utilizing the shockwave from the laser-induced plasma, that were developed in the first project year have been tested in Air Force relevant flow conditions; high-pressure, high-temperature, and supersonic flow conditions.

Figure 18 illustrates the experimental setup used to apply the ns-pulse modulation technique to high-pressure combustion environments. It has been reported that LIBS measurement accuracy gets worse as ambient pressure increases due to the increased collision rate and unstable plasma generation. A few previous studies have suggested the use of shorter pulse width lasers for LIBS under elevated pressure conditions to stabilize the laser-induced plasma and suppress the stochastic inverse-Bremsstrahlung process that intensifies the plasma strength (electron number density). The ns-pulse modulation technique developed in the first

project year can effectively reduce the pulse width, therefore, tested at Air Force relevant high-pressure and high-temperature flow conditions.

A first harmonic 1064nm Nd:YAG laser (Spectra Physics Quanta Ray LAB170) with a repetition rate of 10Hz and constant pulse width of 9.2 ns is used for this experiment. A rotating half-wave plate (HP), placed at the laser outlet, controls the pulse energy (PE), which is set to 230mJ in this experiment. Subsequently, the polarized laser passes through a saturable absorber (SA Innowit Cr:YAG) with normal transmission of 77%. SAs are non-linear optics whose material absorption decreases as the laser power increases, becoming optically transparent to highly energetic laser pulse and opaque to low-intensity radial noise of the laser beam. As a result, the pulse energy downstream of the SA is decreased to 160mJ and 80mJ for each setup. A Galilean beam extender is used to control the irradiance of the beam before it enters the SA, which makes a collimated parallel beam with a reduced cross-section. Then the beam is focused a first time with an f = + 300 mm lens (PCX2) before the transmitted beam is collimated with an f = + 750mm focal length optic (PCX3), thus enlarging the beam diameter from 12 to 30mm, which improves the second or probing plasma stability. The up-and-down-stream temporal beam profile is monitored by two photodiodes (Thorlabs, SM05PD2A, 500-MHz bandwidth) sampling deflected light from the plano-convex lenses. A 1-GHz bandwidth oscilloscope (Keysight, MSO-X 3104A) records the emitted real-time waveform signal. Shot-to-shot fluctuation of the pulse energy is measured to be 2.3% upstream and 4.9% downstream of the chopping plasma. The pulse width of the resulting chopped temporal profile is reduced to 5.0 ns (Fig. 19).

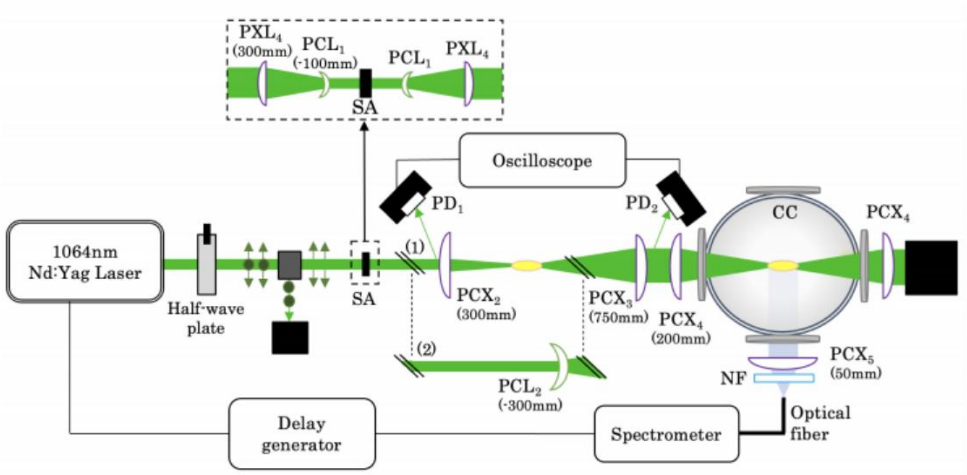

Figure 18 An experimental setup for the application of the ns-pulse modulation technique to high-pressure combustion environments

The modulated laser beam is then focused a second time (PCX4) 15 mm above the exit plane of a flat flame burner. In order to retrieve the original ns-pulse, the first converging lens (PCX2) is replaced with a concave lens (PCL2) to maintain a constant beam diameter in the combustion chamber between the two configurations tested here. The probing scattered light is collected at a 90-degree angle from the laser path by an optical fiber (500 μs in diameter) connected to a spectrometer (Ocean optics USB 2000+). It is synchronized with the Nd:YAG Q-

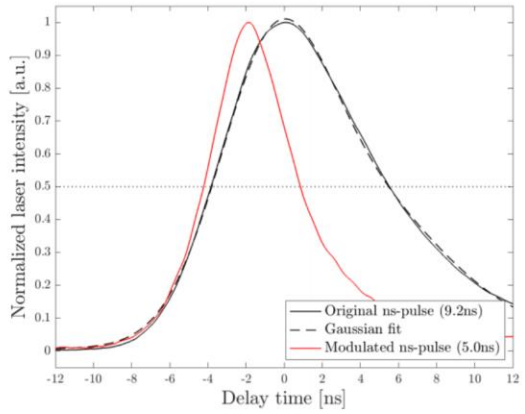

Figure 19 Modulated ns-pulse profile

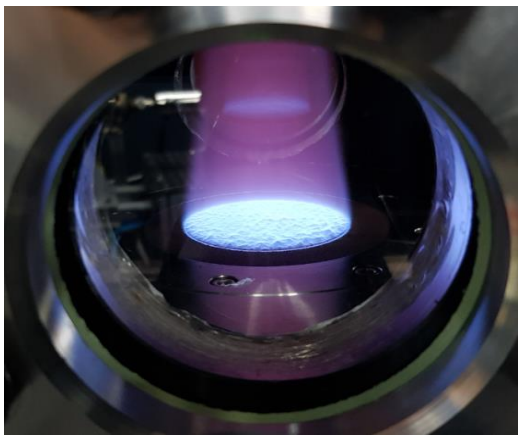

Figure 20 A high-pressure and high-temperature flow generated by McKenna burner installed in a variable-pressure cylindrical chamber (CC)

switch output signal through a delay generator (Stanford Research Systems DG535) set to 90 ms delay. A notch filter (NF) shields the optical fiber from strong 532nm laser emission. The spectral resolution of the USB-type spectrometer is 0.5 nm, scanning from 300 to 800nm with 600 grooves/mm grating.

The lab-scaled high-pressure combustion test facility is installed in a cylindrical chamber (CC) of 180 mm wide by 190mm long casing with four access windows (Fig. 20). Flow rates of the air and fuel are controlled with Bronkhorst mass flow controllers (model F-211AV for fuel and F-112AC for oxidizer). A customized McKenna burner (designed by Holthuis & Associated) of 60 mm diameter is used to generate high-temperature combustion products. The mono-dimensional laminar flat flame on the burner is sensitive to shear flow perturbation thus an outer nitrogen curtain coming from a 6 mm wide porous ring is supplied and minimizes the radial temperature gradients. The sintered plug, center part of the McKenna burner, is equipped with its own cooling system with K-type thermocouples monitoring the water inlet and outlet temperature in real-time, maintaining the surface temperature constant at 298±1K. To ensure the flame location is stabilized 1 mm above the exit plane, a safety factor of 4% is added to the calculated laminar speed.

Figure 21 illustrates the improved measurement (prediction) accuracy of the LIBS with the modulated ns-pulses. POD and kriging model are used for the calibration of the flame emission spectra, and the broadband emission intensity level is reduced with the modulated ns-pulse of reduced pulse width (from 9.6 ns to 5 ns). It was found in our previous study that the stochastic inverse-Bremsstrahlung process can be effectively suppressed by the pulse width reduction, which results in the reduced measurement uncertainty.

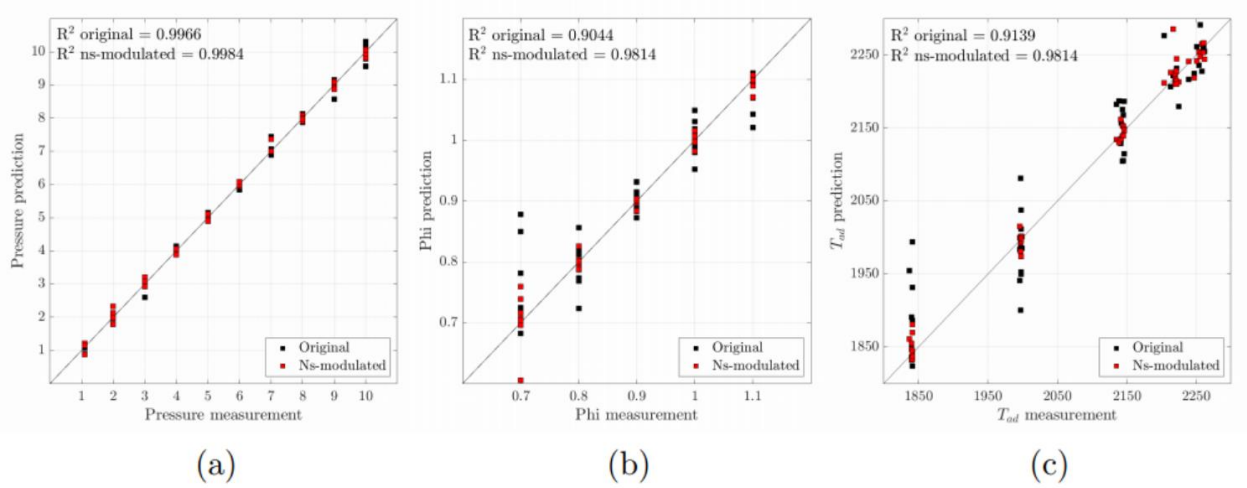

Figure 21 Prediction accuracy of the (a) pressure, (b) equivalence ratio, and (c) adiabatic flame temperature improved by the modulated ns-pulse

High-speed and high-temperature flows are another measurement targets of this research project. Supersonic wind tunnels are used for testing the novel techniques (seedless velocimetry, fast FES, and ns-LIBS) developed in this research project.

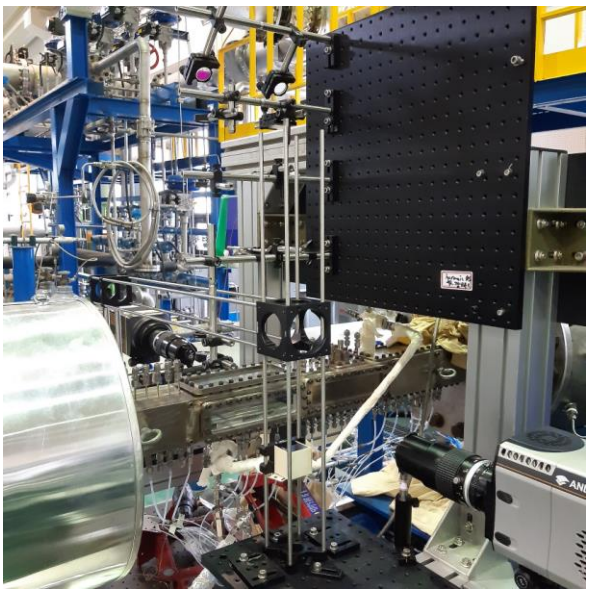

Figure 22 An optical setup for testing the seedless velocimetry technique in a supersonic flow

Figure 22 shows the optical setup designed for the seedless velocimetry in supersonic flows. The automated translational stage carries the optical setup to move the location of the laser-induced plasma along the probe beams. The probe beams are from continuous diode lasers to detect the arrival of the shockwave originating from the laser-induced plasma. The shockwave floating with the ambient flow arrives at the probe beam locations to disturb the probe beam propagation; the time history of the probe beam disturbances is recorded by fast photodiodes. The shock arrival time will merely depend on the ambient flow velocity if the gas composition, density, temperature, laser pulse energy, and the distances between the plasma and the probe beams are fixed. The velocimetry was tested under various supersonic flow conditions to confirm the potential use of the technique in conjunction with the ns-LIBS property monitoring of supersonic flows. It is clear that the flow velocity monitoring is convenient with the addition of light-weight small-size diode lasers and fast photodiodes where a laser-induced plasma is generated for LIBS.

3) A new application of the ns-LIBS for estimating the local combustion efficiency

One of the major limitations of the ns-LIBS comes from the nearly complete dissociation of the molecular species in the plasma. Consequently, identifying parent species is difficult although measurement of molecular species concentration is critical in many situations. Under some Air Force relevant flow conditions in high-speed flows, stabilizing combustion reactions is challenging, therefore, achieving 100% combustion efficiency is impossible. For example, combustor flows need to be supersonic in scramjets to generate positive thrust in hypersonic flights while stabilizing combustion reactions in supersonic flows is challenging. Flame holding in afterburners of turbojets where the flow speed is high is also difficult; wasted unburned fuel has been often observed burning after nozzle during the thrust boosting periods operating afterburners. Therefore, monitoring local combustion efficiency in the high-performance air breathing engines is critical to control and sustain their thrust generation. We plan to monitor the gas properties in combustors using the ns-LIBS, however, it provides only atom concentration information of oxygen (O), hydrogen (H), carbon (C), and nitrogen (N) which are theoretically unchanged by any chemical reactions including combustion. Therefore, combustion efficiency cannot be estimated by the LIBS.

The combustion efficiency can be estimated when concentrations of fuel and molecular oxygen in reactants and combustion products are given or measured. It was shown in our previous studies that the ns-LIBS provides accurate fuel-air ratio in reactants or equivalent fuel-air ratio in combustion products since C, H, and O atom concentrations can be measured calibrating the atomic emission lines in the LIBS spectra or utilizing the POD/ML methods developed in the first project year. The atom concentrations will not be altered by chemical reactions, therefore, molecular species composition in reactants before the combustion reactions can be estimated regardless of the progress of chemical reactions and combustion efficiency if atomic composition of the fuel species is known. Nevertheless, measuring molecular oxygen or fuel species in the combustion products is not possible with the conventional ns-LIBS.

We propose the use of the laser-induced plasma as a continuum light source for measuring the strength of an atomic oxygen absorption line at 777 nm that is highly sensitive to the concentration of molecular oxygen, but not affected by the oxygen atoms consumed in fuel oxidation reactions. In the second project year, it was confirmed that the oxygen atoms contained in major combustion product species such as carbon dioxide and water do not affect the oxygen absorption lines at 777 nm when the absorption line is captured in a very early plasma stage within 10 ns after the laser firing. In and adjacent to the early-stage plasma, the number density of molecular oxygen is still unaffected by the expanding plasma and the plasma-induced shockwave. The small plasma core is extremely hot in a non-equilibrium state to produce photons in a broadband spectral range and the molecular oxygen is quickly dissociated to produce atomic oxygen. However, the dissociation energy of carbon dioxide is much higher than that of molecular oxygen, and the water forms hydroxyl radical plus

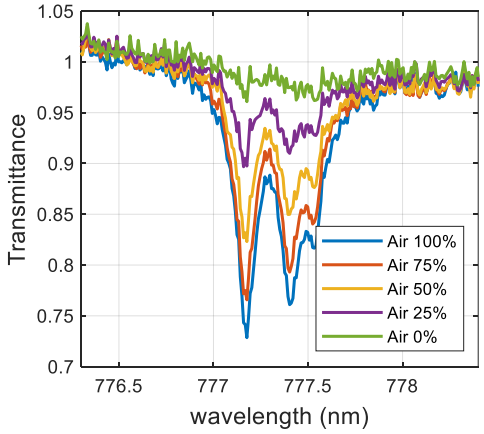

Figure 23 Atomic oxygen absorption line with varied molecular oxygen concentration

atomic hydrogen after the first dissociation, therefore, the concentration of the atomic oxygen from major combustion product species during the early plasma stage is negligible. The strong broadband emission from the plasma core will then be absorbed by the atomic oxygen via the transition of 3s5S0→3p5P at 777 nm. Strong oxygen absorption line is observed as shown in Fig. 8, which is highly sensitive to the molecular oxygen concentration. In Fig. 23, 5 different gas mixtures are prepared to confirm the sensitivity of the absorption lines to the molecular oxygen concentration. Air 100% in the legend means 79% N_2, 21% O_2, and 0% CO_2, and Air 0% is 79% N_2, 0% O_2, and 21% CO_2. As shown in Fig. 23, no oxygen absorption line appears in the gas mixture of 79% N_2, 0% O_2, and 21% CO_2 where the molecular oxygen in air is completely replaced by CO_2. It is evident that 1) the oxygen atoms in CO_2 do not contribute to the photon absorption by the lower energy level atomic oxygen that occurs during the early plasma stage, and 2) the triplet absorption line strength is highly sensitive to the molecular oxygen concentration before the optical breakdown. It is noteworthy that gas mixtures containing H_2O were also tested, and no contribution of H_2O to the absorption lines was confirmed.

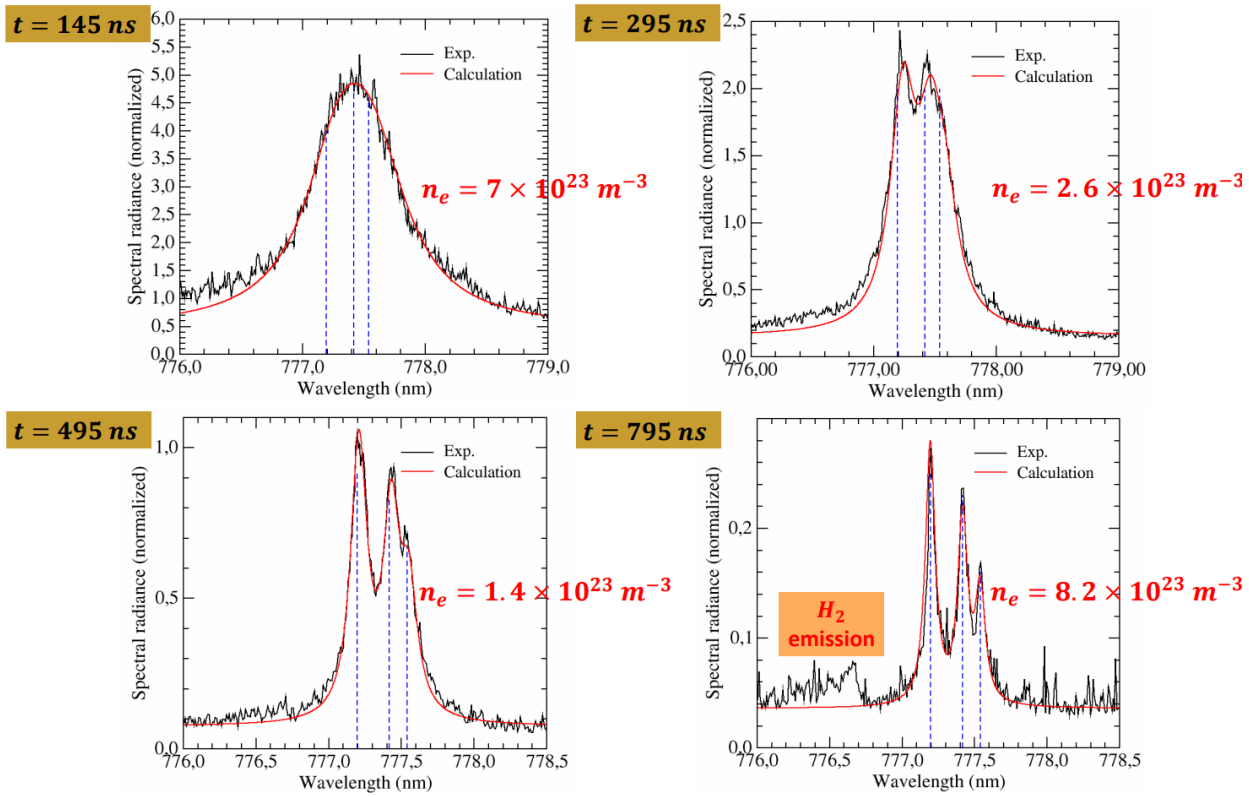

Figure 24 Oxygen triplet emission lines at 777 nm captured later than 100 ns from the laser firing (AURÉLIEN FAVRE et al. 12th Serbian Conference on Spectral Line Shapes in Astrophysics, Vrdnik, SERBIA, June 3-7, 2019)

Figure 24 describes the time evolution of the triplet oxygen emission lines observed during the later stage of the laser-induced plasma. The dissociated oxygen atoms in the plasma-induced high-pressure region collide frequently to broaden the triplet emission lines which are completely merged at 145 ns after the laser firing. Then the line width gets thinner as the

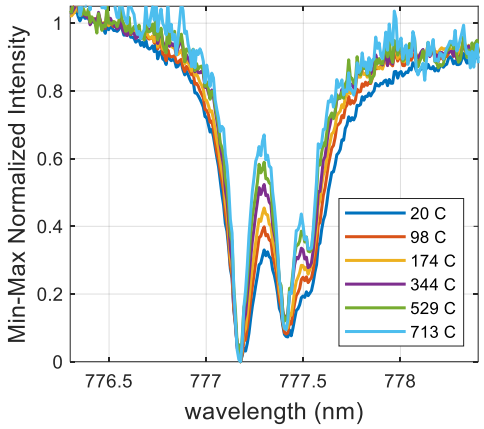

Figure 25 Oxygen triplet absorption line

pressure relieves and the plasma expands to make the triplet lines clearly separated. Obviously, similar absorption line structures are observed in Figs. 23 and 25. Since the absorption lines are captured in the earliest stage of the plasma, initial gas conditions, e.g., the gas density and temperature, will significantly affect the spectrum profile. Figure 25 shows the line broadening of the absorption lines as the gas density increases, or temperature decreases. At the highest temperature (713 °C) thus the lowest initial gas density, the oxygen triplet absorption lines are clearly separated while they merge as the temperature decreases. This indicates that the width of the absorption lines can serve as a temperature (at a fixed ambient pressure) or gas density indicator. Nevertheless, it was found that the signal to noise ratio (SNR) gets worse as the gas density decreases or the temperature increases at a fixed pressure condition. This is because the plasma strength and the continuum radiation from the plasma core in the early stage are weaker at lower gas density conditions. Raising the laser pulse energy would improve the SNR, however, it will cause greater disturbances when the plasma is generated in reactants. Alternatively, preceding UV laser pulses can generate seed electrons to stabilize the following breakdown at low density conditions, which was confirmed in our preliminary experiments. To apply this technique to Air Force relevant turbulent combustion conditions where the gas density fluctuation is significant, the UV guided stable plasma generation technique has been investigated in the third project year while it adds system complexity.

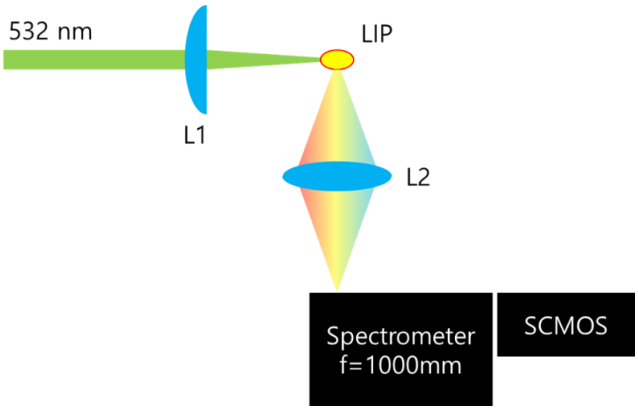

Figure 26 The simplest optical setup for proposed method measuring local combustion efficiency

When this method is combined with conventional ns-LIBS, local combustion efficiency in high-speed combustors can be quantified. Recall that the equivalence ratio before the combustion reactions to occur can be accurately measured utilizing the plasma emission spectra captured in a later plasma stage. From a single laser-induced plasma, two spectra will be captured separately at two different gate delays; the earlier exposure is to capture the oxygen absorption line for measuring molecular oxygen concentration, and the later one is for conventional LIBS to estimate local equivalence ratio.

One of the best merits of the technique is the simplest optical setup (Fig. 26). Second harmonic pulses of a Nd:YAG laser at 100 mJ/pulse are focused to the gas samples by a focusing lens (L1 in Fig. 26) for generating a laser-induced plasma. Then photon emission from the plasma is collected from the right angle and guided onto the slit of a high-resolution spectrometer (Acton Research AM-510, f = 1000mm, 0.015 nm/pixel). The spectrum is recorded

by a nanosecond gated high-speed camera at 4 ns after the onset of the optical breakdown with 4 ns gate width.

5. YEAR-3 RESULTS

1) Measurements in air force relevant flow conditions

Highly turbulent, high-speed, high-temperature, and high-pressure flows are essential for high-performance propulsion systems that the air force has developed for various purposes. The optical measurement techniques developed for the first two project years have been tested under such harsh flow conditions. One of the most challenging measurement environments can be found in high-pressure swirl-stabilized combustors. Under the high-pressure and high-temperature turbulent flow conditions, quantifying gas properties is difficult since most conventional sensors are inapplicable. Figure 27, a picture of an overheated high-pressure swirl-stabilized combustor, well describes the difficult measurement environment where the combustor housing can frequently be overheated damaging the sensors attached on it. The high-pressure test condition makes optical measurements difficult as well with the significant surface emission, broadening of emission-absorption lines, refracting laser beams and light rays, and damaging optical windows. In addition, the fast fluctuation of the gas density field will significantly raise the measurement uncertainty of n-LIBS since the breakdown location is strongly dependent on the gas density near the focal volume.

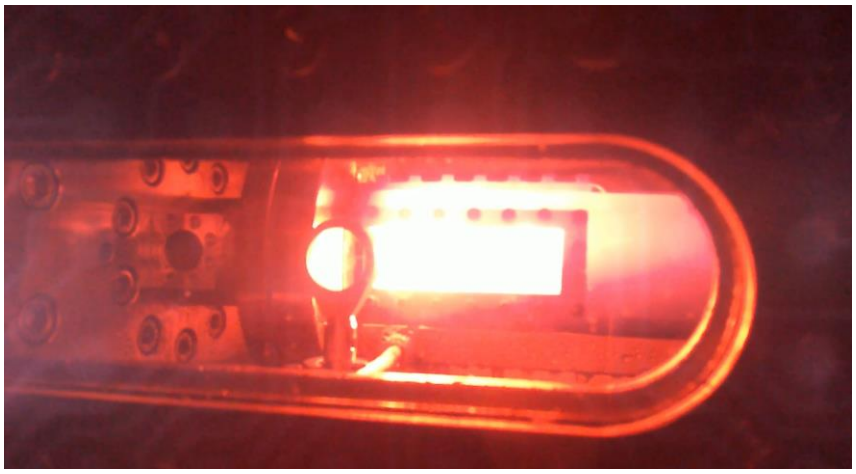

Figure 27 Overheated high-pressure swirl-stabilized combustor at 20 bar

The novel LIBS technique developed in the first two project years is tested in a high-pressure swirl-stabilized turbulent combustor. The combustor is designed to simulate a gas turbine combustor that can be used for turbojet engines and power generation systems. Nominal operation condition of the combustor is 20 bars as in typical gas turbine engines. Swirling strength of the combustor is variable and the swirl vane is conveniently replaceable. Hydrogen is added to methane fuel up to 50% to test the fuel flexibility of the combustor. The same optical setup illustrated in Fig. 18 was used for the experiments. The 1024 nm laser pulses from a Nd:YAG laser is first focused outside of the high-pressure combustor to generate a chopping plasma cutting the trailing edge of the laser pulse to reduce the pulse width from 9 ns to 5 ns. Due to the reduced pulse width, the size of the laser-induced plasma in the combustor decreases with improved breakdown stability. As previously investigated, the IB-induced continuum

emission is weakened, and the measurement accuracy is improved. POD and kriging model are used to reduce the order of the spectrum data and calibrate the spectra with fuel concentration, pressure, and gas density.

Figure 28 Typical high-P flame in a heated quartz liner

Figure 28 shows a typical high-pressure flame in a quartz liner. The fluorescence of the heated quartz makes the emission measurement difficult, however, LIBS signal is strong enough to dominate the fluorescence for a short exposure. The high-temperature combustion environment is particularly challenging because of the fast gas density fluctuation as previously mentioned. Pure hydrogen combustion is recently regarded as an environmental-friendly energy conversion method. However, the hydrogen combustion reaches even higher temperature than other hydrocarbon flames and the flow speed should be higher to stabilize the fast hydrogen flames. Under a pure hydrogen flame test condition where the unburned gas flow speed is 30 m/s and overall equivalence ratio is approximately 0.7, 2D LIBS measurement is attempted. We chose to estimate the density field only using the plasma energy calibrated with the gas density, thus, temperature with pressure information. Figure 29 shows the temperature profile measurement results in the hydrogen combustor. As expected, the local temperature exceeds 2,500K which is higher than that seen in typical hydrocarbon flames.

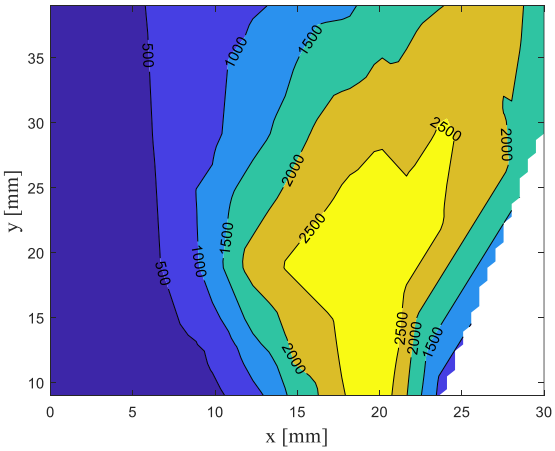

Figure 29 Temperature field estimated with the ns-LIBS in a pure hydrogen flame at 30 m/s unburned gas velocity and 0.7 overall equivalence ratio

2) Two separate emission spectra captured at two different delays

As invested in the previous project years, the property information that can be extracted from the plasma emission spectra is different depending on the delay and exposure time after the breakdown of the laser-induced plasma. For example, oxygen absorption lines appear only when

the strong continuum emission, presumably from the hot electrons, remains dominant during the early stage of the laser-induced plasma; the oxygen absorption line intensity indicates molecular oxygen concentration prior to the breakdown. However, atomic emission lines are submerged in the continuum radiation during the early plasma stage. Recall that the species concentration information is from the atomic emission lines as shown in the previous investigation aided by the POD, which confirms that the bases consisting of the atomic emission lines determine the species composition. Nevertheless, the atomic lines do not contain molecular information, therefore, the oxygen absorption lines should be separately captured; therefore, two-delay LIBS measurement is tested in this study. Figure 30 illustrates an optical setup for the two-delay LIBS measurements in a supersonic combustor.

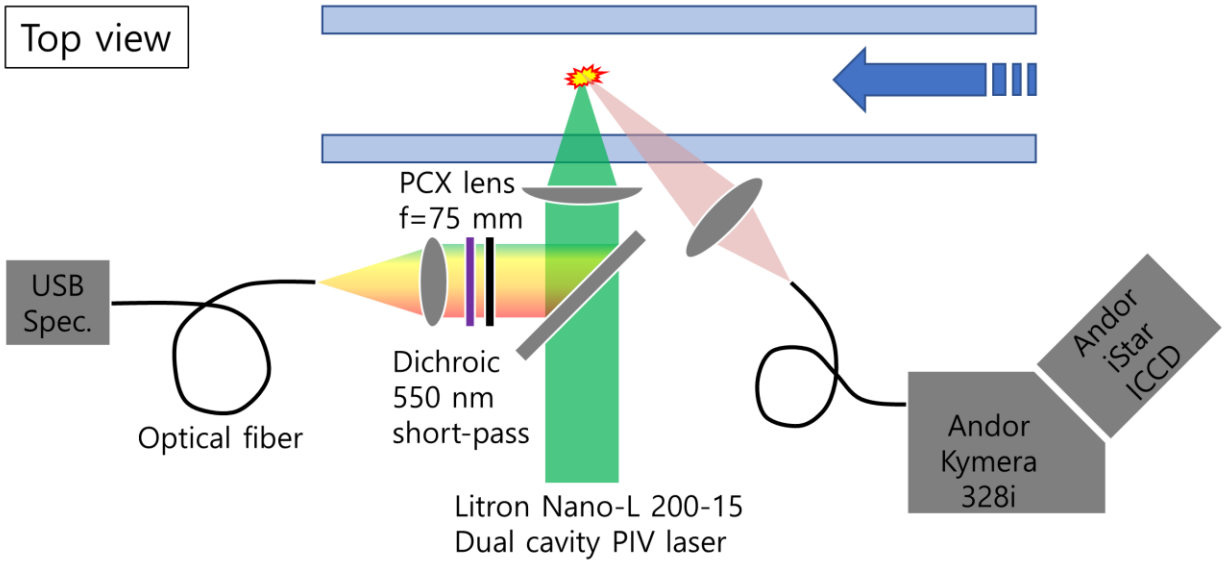

Figure 30 A schematic diagram of an optical setup for two-delay LIBS measurements in a supersonic combustor (the blue arrow in the flow channel indicates the direction of the supersonic flow, Ma = 2.5)

The two-delay LIBS measurement requires two separate sets of photon detection systems, and one of the two should have a signal intensifier to capture the oxygen absorption lines that survive only for a short period of time, 2 – 6 ns after the breakdown. A high-resolution spectrometer with an ICCD camera at the exit plane of the spectrometer is used to record the oxygen absorption line as in the calibration experiments conducted in the second project year. The other spectrometer system records the atomic-line-dominated plasma emission spectra that are easy to collect since the rest of the photon emission period would mostly be dominated by the atomic emission lines. Therefore, a USB-type portable spectrometer is used for this purpose. A dichroic (550 nm short-pass) mirror is used for transmitting the 532 nm laser from a compact PIV laser (Litron Nano Series) while reflecting the plasma photon emission toward the USB-type spectrometer. A separate photon collection for the oxygen absorption line measurement is from an upstream direction. Both the photon collections are from the backscattering direction to minimize the influence of the fluctuating breakdown location along the laser beam propagation direction in the non-uniform high-speed compressible flow conditions.

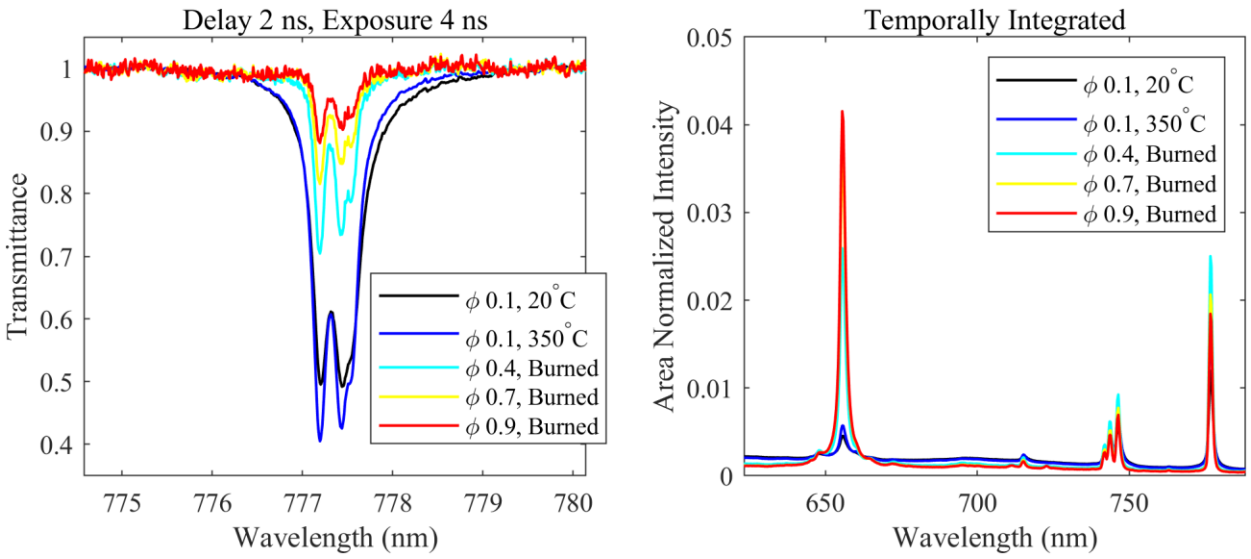

Figure 31 Two-delay LIBS measurement results

Figure 31 shows the spectra captured with the two different delays under the conditions where the flow temperature is accurately controlled, and the combustion efficiency is nearly 100%. The oxygen absorption lines are collected from 2 – 6 ns by a high-resolution spectrometer (1,000 mm focal length) during the continuum dominated time, and the atomic emission lines are collected after the breakdown for a much longer period using the USB-type spectrometer. It is clear that the oxygen absorption lines are highly sensitive to the molecular oxygen concentration, i.e., number density, therefore, decreases as the combustion reaction consumes the molecular oxygen. It was previously confirmed in the second project year that the oxygen absorption intensity is insensitive to the concentration of carbon dioxide and water. In addition, the atomic emission lines captured by the USB-type spectrometer (right in Fig. 31) is highly sensitive to the fuel concentration. In conclusion, the two-delay LIBS can be used for simultaneous measurements of molecular oxygen concentration and fuel concentration.

Another tests with a lower resolution spectrometer (300 mm focal length) are conducted for reducing the size of the measurement system, however, it is found that the triplet oxygen absorption lines should be clearly resolved for utilizing the POD aided calibration. Figure 32 shows the two-delay LIBS spectra with the lower resolution spectrometer, and the oxygen absorption lines are unclear to be used for quantitative measurements. Without the spectra delineating the oxygen triplet structure, calibration accuracy becomes remarkably worse, and the low signal-to-noise ratio makes the intensity estimation difficult. In short, molecular oxygen measurement with the ns-LIBS requires high-resolution spectrometer system with a signal intensifier, therefore, it is inappropriate for a compact measurement system when considering onboard applications.

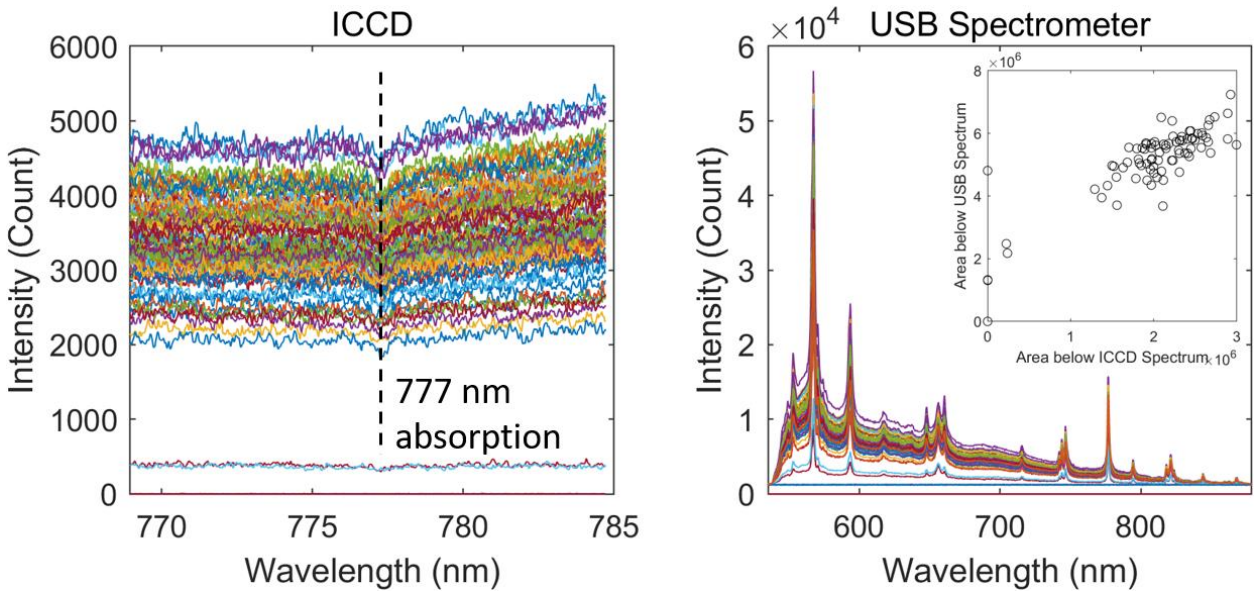

Figure 32 Oxygen absorption lines and atomic-line-dominated spectra captured in the supersonic combustor with reduced spectral resolution

3) Low pulse energy gas property measurements

In order to reduce the laser energy requirement of the gas property measurement system, spontaneous Rayleigh-Brillouin scattering (SBRS) is investigated to measure gas species and density without laser-induced breakdown. For the LIBS measurements, focused laser pulses should have relatively high energy above the breakdown threshold for inducing plasmas near the focal volume. On the other hand, the laser-induced scattering, e.g., Mie, Rayleigh-Brillouin, and Raman, occurs at comparably lower laser energy as its threshold is set to trigger the dipole-induced motion of polarizable gas molecules. The scattering signals contain gas property information as well, therefore, a microchip or DPSS-type compact laser with a narrow spectral width can be used for the gas property measurements. However, high-resolution spectral dispersion is required to extract the quantitative gas property information from the scattering signals. A compact transmissive spectrometer, e.g., Fabry-Perot etalon (FPE), can provide high enough spectral resolution when aided by intensified photon detectors such as ICCD and PMT.

Polarized incident photons from a laser can align dipoles of polarizable gas molecules, and the molecules will exhibit single and bulk motions responding to temperature and pressure fluctuations, respectively. These fluctuations alter local refractive index which depends on the dielectric constant of gas medium. As a result, photons are scattered in a way meeting the Bragg condition, while their frequency shifts depend on the type of molecular motion. In the spectral domain, a Rayleigh peak from a single molecular motion with temperature broadening, i.e., Doppler broadening, would be centered without spectral shift. On the other hand, Brillouin sidebands from photon-phonon interactions with a group of molecules behave as acoustic phonons residing on sound waves, and the scattered photons undergo Stokes/anti-Stokes shifts to be equally spaced from the center in spectral domain. Consequently, physical information, e.g., transport/thermodynamics properties of gas molecules, is contained in the spectral structure of the SRBS signals.

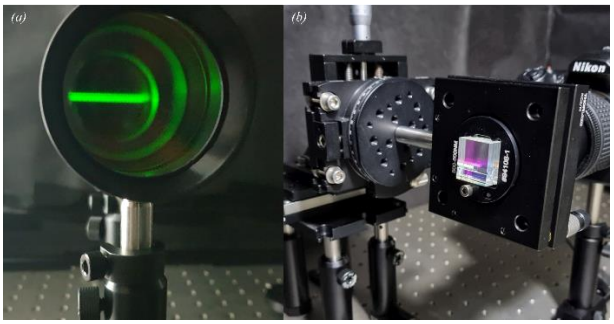

Figure 33 (a) Laser-induced Rayleigh-Brillouin scattering captured by μs-order exposure time, and (b) virtually imaged phased array mounted on a rotation mount for angular tuning.

The non-coherent SRBS utilizes (I) a compact optical setup with a single low-energy photon source, and (II) the signal acquisition angle is unlimited although (III) the signal is unstable compared to coherent RBS (CRBS). As the SRBS propagates along the plane of the polarization of incident photons, frequency conversion by the spectral disperser keeps the original spatial information that depends on the dispersion direction. A virtually imaged phased array (VIPA) is a kind of single-body solid FPE's with angular tunability guaranteeing parallelism between the facing optical surfaces reflecting photons, which induces one-dimensional domain conversion while the residual domain remains as the original spatial domain. Therefore, the VIPA is more compact than typical spectrometers using reflective gratings and works better to resolve spatial property distribution of interacting gas molecules along the loosely converging laser beam causing the SRBS. The auxiliary spherical lens, which is installed behind the VIPA, focuses dispersed photons in constructive interference modes, therefore, the resultant fringe patterns on the object plane are circularly distorted maintaining 1D spatial information.

The SRBS signal is inherently unstable, primarily due to the shot-to-shot instability of pulsed laser systems, because there is no coherent optical lattice as in CRBS. Therefore, high order signals should be taken to remove the property-irrelevant noise sources, and signal decomposition, e.g., proper orthogonal decomposition (POD), is essential to extract reduced-order coefficients via projecting original SRBS signals on a space spanned by selected principal bases. Then the POD coefficients and corresponding signal intensity spectrally integrated, which represent spectral structure and scattering cross-section, respectively, as previously proposed by Miles et al., are used for multi-property calibration. The calibration comprises gas species classification and density regression utilizing a support vector machine (SVM). The SVM adjusts optimal hyperplane between classifiable data maximizing margins and allowable error boundaries for appropriate regression. The number of POD coefficients is chosen based on the signal reconstruction accuracy and evaluation parameters, e.g., accuracy (ACC_{test}) and correlation coefficient (R^2) for the classification and regression, respectively. Figure 34 shows the density calibration curves with different gas species utilizing the SRBS signals.

In conclusion, the SRBS can be used for gas species and density measurements without inducing plasmas that require high laser pulse energy.

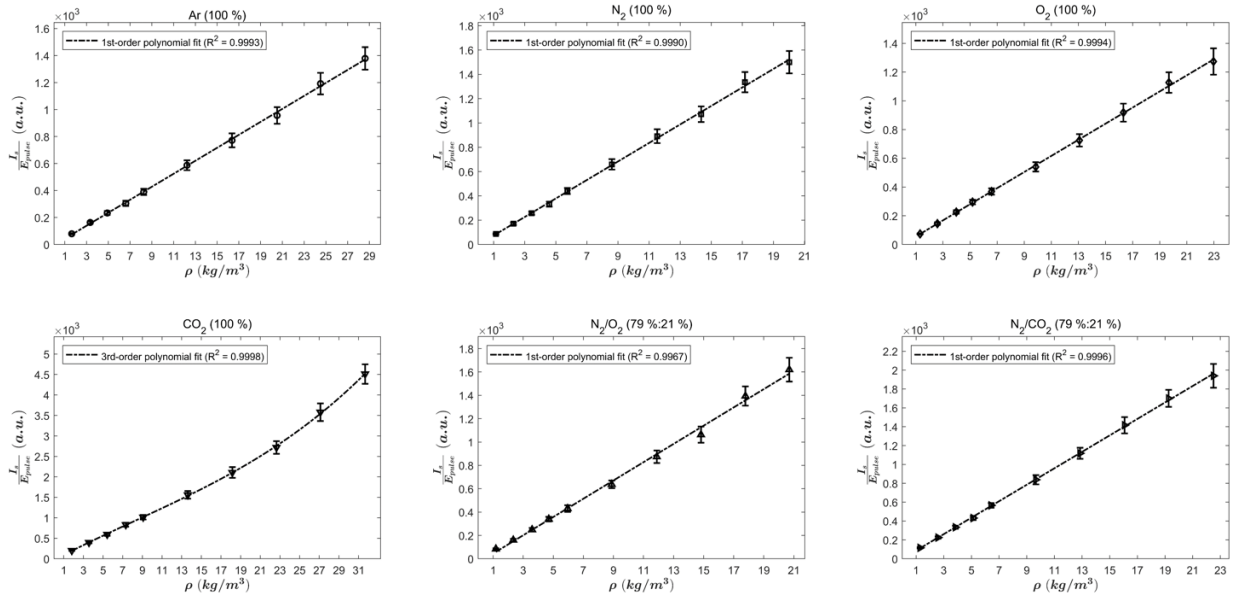

Figure 34 SRBS calibration results with varied gas species and density

6. SUMMARY

The original design of the gas property monitoring system is illustrated in Fig. 1. There are two separate measurement domains considered for the design; (1) Cold (unburned) Flow Region and (2) Hot (burned) Flow Region.

In the Region (1), ps-LIBS or chopped ns-LIBS is proposed for measuring the gas density, species concentration, and velocity in the intake and isolator area since there is no photon source (within UV, VIS, and NIR for easy detection) in cold flows. For improving the accuracy and extending the possible measurement conditions of the ns-LIBS, the ns laser pulses are modulated, and data-driven machine learning techniques are employed. However, the LIBS measurement inherently requires relatively high laser pulse energy for inducing the breakdown. In addition, a diode laser with a set of guide optics is essential for the velocity measurement using LIBS as tested in the first project year. Interestingly, particularly in the supersonic flows, the SRBS signal is found to be sensitive to the flow speed, therefore, the SRBS signal can also be used for estimating the flow velocity although the LIP-induced shockwave velocimetry (LIPSV) developed in the first project year is more accurate velocity measurement method. We will continue to improve the SRBS velocimetry in a future work. The SRBS signal is fine resolved by a minimal-sized VIPA to be calibrated with gas density and discern molecular species. It is shown that, at least with a limited number of molecular species, the SRBS can be used for gas density and composition measurements. In short, the measurement system in the Region (1) can be further simplified with the SRBS method implemented with a low power laser source, a minimal-sized VIPA optics, and a 2D CCD array chip, e.g., a quarter square inch panel for 1024 by 1024 pixels, to image the 2D SRBS signal.

In the Region (2), the flame emission spectroscopy (FES) aided by the POD calibration and physics-guided denoising CNN is proven to be the simplest and accurate gas property monitoring

method in the combustion region. The spontaneous photon emissions from the reaction regions contain such quantitative property information, and a miniaturized small spectrometer is found to be sufficient to capture the flame emission characteristics. Therefore, a tiny spectrometer with a data processing unit would be enough to provide the combustor operation conditions essential for vehicle control, which includes local fuel concentration, flame temperature, and gas density. Local concentration of molecular oxygen could also be measured using the two-delay LIBS developed in this research project, that records oxygen absorption lines in the early plasma stage later with the atomic emission lines. Nevertheless, the oxygen absorption line measurement requires a high-resolution spectrometer of a long focal length with a signal intensifier. Therefore, the two-delay LIBS is inappropriate for the onboard system although the absorption spectroscopy is an effective method estimating molecular oxygen concentration indicating local combustion reaction progress.

Consequently, the proposed gas property measurement system consists of 1) a tiny single optical access or optical cable for each of the inlet-isolator and engine, 2) a portable low-resolution spectrometer for FES, 3) a low-power laser source inducing SRBS, 4) minimal-sized VIPA optics set, 5) a CCD array chip, and 6) a signal processor converting the optical signals to the gas properties of interest including I) density (temperature with pressure information), II) gas composition, and III) velocity. Among the various optical measurement methods tested in the research project, 1) fast FES with POD-guided Machine Learning & Denoising and 2) SRBS are chosen for the onboard gas property monitoring system.

5. PUBLICATIONS

1. Seon Woong Kim, Jongwun Choi, Hosung Byun, Taekeun Yoon, Campbell D. Carter, Hyungrok Do, “Detection of molecular oxygen using nanosecond-laser-induced plasma,” Optics Express Vol. 31, Issue 20, pp. 32504-32515 (2023)

2. Juhyun Bae, Hosung Byun, Taekeun Yoon, Campbell D. Carter, Hyungrok Do, 2021, “Novel calibration-free seedless velocimetry using laser-induced shockwave,” Experimental Thermal and Fluid Science 126: 110384

3. H. Byun, J. Bae, T. Yoon, I. Yang, S. Lee, C. D. Carter, H. Do, 2022, “Velocity measurements in a supersonic wind tunnel with a novel calibration-free seedless velocimetry utilizing laser-induced shockwaves and a double-line probe system,” Int. J. Heat and Mass Transfer 184: 122246

4. T. Yoon, S. W. Kim, H. Byun, Y. Kim, C. D. Carter, and Hyungrok Do, 2022, “Deep learning-based denoising for fast time-resolved flame emission spectroscopy in high-pressure combustion environment,” submitted to Comb. Flame